Energy-Exchange Effects in Few-Particle Coulomb Scattering

Jamal Berakdar

Atomic and Molecular Physics Laboratories, Research School of Physical Sciences and Engineering, Australian National University, Canberra, ACT 0200, Australia

(Received 30 September 1996)

For the description of an arbitrary nonrelativistic three-body Coulomb system an analytical approximate wave function is designed which is correct for large interparticle separations. At shorter distances, where the potential energy dominates the kinetic one, the wave function is a linear mixture of products each consisting of three two-body Coulomb waves propagating *off the two-body* energy shell but *on the total* energy shell. The method is employed for the calculations of multiply differential cross sections for photo-double ionization of helium and for electron, positron, proton, and antiproton-impact ionization of atomic hydrogen. [S0031-9007(97)02917-7]

PACS numbers: 32.80.Fb, 34.10.+x, 34.80.Dp

The description of the correlated dynamics of few charged particles is one of the fundamental unsolved problems in atomic, molecular, and nuclear physics. In addition to the inherent nonseparability of many-body interacting systems, the infinite range of the Coulombic interaction poses a severe obstacle in theoretical treatments. For example, in resonant or direct fragmentation processes involving charged particles the long-range tail of Coulomb forces precludes free asymptotic states of the reaction fragments [1–4], which in turn seriously limits the applicability of standard methods of scattering theory. While the complicated dynamical nature of asymptotic Coulombic states has been unraveled in recent years [1–4], our knowledge of the fragmentation dynamics at finite interparticle distances is still scarce, in particular, if the strength of the different interactions involved is of the same order and a perturbative approach is inappropriate. An adequate description of the short-range dynamics is, however, imperative, since dissociation amplitudes involve the many-body scattering state in the entire Hilbert space.

This study aims at modeling the reaction dynamics of three arbitrary charged particles at finite interparticle separations while maintaining the requirement of exact treatment at infinite interparticle distances. For this purpose, following Refs. [5,6], we split the Hilbert space into an "inner" and a "far zone" depending on whether the total potential is larger or smaller than the kinetic energy. The scattering state in the inner zone is designed with special regard to the fragmentation dynamics. Subsequently, this state is mapped onto the asymptotic solution at the boundary between the inner and the far zone to arrive at an asymptotically correct behavior. Here we operate in a nonrelativistic time-independent framework. To decouple kinematic from dynamical properties we write the eigenfunction Ψ of the total Hamiltonian $\mathcal{H}$, at the total energy E, in the form (atomic units are used throughout)

$$\Psi(\mathbf{r}_{ij}, \mathbf{R}_k) = N \exp(i\mathbf{r}_{ij} \cdot \mathbf{k}_{ij} + i\mathbf{R}_k \cdot \mathbf{K}_k)\overline{\Psi}(\mathbf{r}_{ij}, \mathbf{R}_k), \tag{1}$$

where $\mathbf{k}_{ij}$ denote the momenta conjugate to the interparticle distances $\mathbf{r}_{ij}$, while $\mathbf{R}_k$ refers to the position of particle k with respect to the center of mass of the pair ij. $\mathbf{K}_k$ designates the momentum conjugate to $\mathbf{R}_k$, and N is a normalization factor. The distortion $\overline{\Psi}(\mathbf{r}_{ij}, \mathbf{R}_k)$ is solely due to the presence of the total potential. It can be determined as an eigensolution of an operator H whose properties are most transparent when expressed in the curvilinear coordinate system

$$\{\xi_k = r_{ij} + \hat{\mathbf{k}}_{ij} \cdot \mathbf{r}_{ij}; \xi_m = r_{ij}\},$$
$$\epsilon_{ijk} \neq 0; \quad j > i, k \in [1,3]; \quad m \in [4,6]. \tag{2}$$

In terms of (2) H decomposes into two *parametrically* coupled differential operators; an operator H_{par} which is differential in the *parabolic* coordinates $\xi_{1,2,3}$ only and an operator acts only on internal degrees of freedom r_{ij} [4]. An additional mixing term arises from the off-diagonal elements of the metric tensor. The parabolic operator H_{par} is exactly separable in the coordinates $\xi_{1\ldots3}$ for it factorizes as

$$H_{\mathrm{par}} = \sum_{j=1}^{3} H_{\xi_j}, [H_{\xi_j}, H_{\xi_i}] = 0; \quad \forall\, i, j \in \{1,2,3\}, \tag{3}$$

where

$$H_{\xi_j} = \frac{2}{\mu_{lm} r_{lm}} [\partial_{\xi_j} \xi_j \partial_{\xi_j} + i k_{lm} \xi_j \partial_{\xi_j} - \mu_{lm} Z_{lm}];$$
$$\epsilon_{jlm} \neq 0, \quad j \in \{1,2,3\}. \tag{4}$$

In Eq. (4) μ_{ij}, Z_{lm} denote the reduced mass of the pair ij and their product charge, respectively. Equation (4) is the Schrödinger equation for two-body Rutherford scattering expressed in parabolic coordinates [7]. Hence, within $H \approx H_{\mathrm{par}}$, the three-body system is considered as the sum of three spatially decoupled two-body Coulomb systems on the *two-body energy shell* $E_{ij} = k_{ij}^2/2\mu_{ij}$. The exact regular eigenfunction of the operator H, within $H \approx$

 0031-9007/97/78(14)/2712(4)$10.00

$H_{\rm par}$, has thus the explicit form (outgoing wave boundary conditions are assumed)

$$\overline{\Psi}_{\rm par}(\xi_{1\cdots6};\mathbf{k}_{ij}) = {}_1F_1(i\beta_{23},1,-ik_{23}\xi_1) \times {}_1F_1(i\beta_{13},1,-ik_{13}\xi_2) \times {}_1F_1(i\beta_{12},1,-ik_{12}\xi_3). \quad (5)$$

Using Eq. (1), the eigenstate $\Psi_{\rm par}$ of $\mathcal{H}$ is then readily deduced. The Sommerfeld parameters β_{ij} are given by $\beta_{ij} = Z_{ij}\mu_{ij}/k_{ij}$. The asymptotic separability ($\lim_{\xi_{1,2,3}\to\infty} H \to H_{\rm par}$) and the parametric dependence of H_{ξ_j} [Eq. (4)] on internal degrees of freedom can be exploited to introduce coupling between the two-body subsystems [4]. This approach, however, does not account for transitions into intermediate virtual states and is applicable only to two electrons moving in the field of a residual ion [8]. To circumvent these shortcomings we adopt a strategy which is motivated by the measurement process and the analysis of Refs. [5,9]. In a scattering experiment the measurable quantities (observables) are the *asymptotic* momenta $\mathbf{k}_{ij}$ of the emerging reaction fragments (spin and spatial degrees of freedom are considered to be decoupled). In the "reaction zone" these quantum numbers are undetermined. To quantify this picture we define an inner, *momentum-exchange zone* and an outer, *asymptotic zone* depending on whether the total potential or the kinetic energy is the dominant quantity. As is well known [5,6], the boundary between these regimes is the Wannier radius R_w which is a scalar quantity. In the inner zone a two-body subsystem ij can assume any two-body quantum state defined by a particular $\mathbf{k}'_{ij}$, i.e., each two-body subsystem propagates *off the two-body energy shell* E_{ij}. The description of this is well facilitated by Eqs. (3)–(5) since the momenta $\mathbf{k}_{ij}$ enter in Eqs. (4) as dummy parameters and are determined only in the outer asymptotic zone where they are measured. To ensure the invariance of the Schrödinger equation under the introduction of intermediate momenta $\mathbf{k}'_{ij}$ we must operate under the constraint that the total energy E is conserved, i.e., the two-body subsystems exchange an indefinite amount of momentum in the momentum-exchange zone and virtually occupy all (two-body) continuum states available in the energy band $[0,E]$. As the system evolves towards the Wannier boundary R_w the reaction fragments take on the (asymptotic) momenta measured in a scattering reaction. In this model the directions $\hat{\mathbf{k}}_{ij}$ are fixed by the boundary conditions [see Eq. (2)]. The exact (regular) eigenfunctions $\Psi_{\rm par}$ of $\mathcal{H}$ (within $H \approx H_{\rm par}$) are known and characterized by k'_{ij}, with $E'_{ij} \in [0,E]$. The general solution in the inner zone is a linear superposition of $\Psi_{\rm par}(\xi_{1\cdots6};k'_{ij})$,

$$\Psi^{\rm in}(\xi_{1\cdots6}) = \mathcal{N}\int d^3\mathbf{k}'_{ij}\, d^3\mathbf{K}'_k\, A_{\mathbf{k}'_{ij}}\Psi_{\rm par}(\xi_{1\cdots6};\mathbf{k}'_{ij}) \times \delta(E-E')\delta^2(\hat{\mathbf{k}}_{ij}-\hat{\mathbf{k}}'_{ij})\delta^2(\hat{\mathbf{K}}_k-\hat{\mathbf{K}}'_k), \quad (6)$$

where E' is the intermediate total energy. Since $\Psi^{\rm in}$ is a linear combination of eigenstates of $\mathcal{H}$ (within $H \approx H_{\rm par}$) it is obvious that $(\mathcal{H}-E)\Psi^{\rm in} = 0$. To account for the neglected part $H - H_{\rm par}$ the expansion coefficients $A_{\mathbf{k}'_{ij}}$ have to be deduced, e.g., variationally. For many-body continuum states, however, this procedure is intractable. Here only the low-energy part of $A_{\mathbf{k}'_{ij}}$ is needed since the wave function (6) is defined only in the inner, momentum-exchange zone whose boundary (R_w) scales inversely with E [6]. Within our model the expansion coefficients $A_{\mathbf{k}'_{ij}}(\xi_{4\cdots6})$ indicate the occupation probabilities for the intermediate states characterized by $E'_{ij} \in [0,E]$. According to the Wannier threshold analysis [5], the correlated motion in the interaction region is ergodic and hence our assumption $A_{\mathbf{k}'_{ij}}(\xi_{4\cdots6}) = 1$. At the boundary R_w the function $\Psi^{\rm in}$ has to be mapped onto the asymptotic state (5), which can be done as in the R-matrix approach [9]. Here we smoothly connect $\Psi^{\rm in}$ with the asymptotic states (5) at R_w by writing the three-body state in the entire Hilbert space in the form

$$\Psi_{\rm ex}(\xi_{1\cdots6};E) = f\Psi^{\rm in} + (1-f)\Psi_{\rm par}(\xi_{1\cdots6};\mathbf{k}_{ij}), \quad (7)$$

where $f := \exp(-R/R_w)$ is an exponential matching factor and $R := r_{12} + r_{13}$ measures the extent of the three-body system. Since R_w and R are scalar quantities, i.e., they depend on $\xi_{4\cdots6}$ only, the wave function $\Psi_{\rm ex}(\xi_{1\cdots6};E)$ is an eigensolution of the total Hamiltonian within the approximation $H \approx H_{\rm par} = \sum_{j=1}^{3} H_{\xi_j}$. As $\Psi_{\rm par}$ is asymptotically correct for large interparticle separations [2,4] and satisfy the Kato [10] cusp conditions [4] (R is always large in this case) it follows that these properties are directly reflected into $\Psi_{\rm ex}$ ($\lim_{R\gg1} f \to 0$). For $R \gg R_w$ we fall back to Eq. (5); i.e., in a high-energy scattering ($R_w \propto 1/E \to 0$) the escaping particles directly assume their experimentally measured momenta. For $R < R_w$ the two-body subsystems exchange an indefinite amount of energy. At low energies R_w extends to very large distances. The three particles then exchange energies up to infinity for $E \to 0$ and the transformation of the total wave function from $\Psi^{\rm in}$ to $\Psi_{\rm par}$ occurs at very large distances. This implies that properties of scattering amplitudes which are derived from asymptotic arguments are smeared out at threshold. If the integral in Eq. (7) runs over virtual bound states as well, highly excited Rydberg states provide, at lower energies, the major contribution to the wave function $\Psi_{\rm ex}$. If the Hamiltonian $\mathcal{H}$ contains short-range (nuclear) interactions, the second term of Eq. (7) remains unchanged while the signature of these interactions is carried by $\Psi^{\rm in}$.

In a reaction leading to three-body continuum states scattering amplitudes are determined by transition matrices of the form (prior form) $T = \langle\Psi_{\rm ex}|W|i\rangle$, where $|i\rangle$ is the initial state of the three-body system and W is the perturbation operator due to which the final state $\Psi_{\rm ex}$ is achieved. Introducing hyperspherical momenta $\kappa = E'$; $\tan\alpha = (K'_k/k'_{ij})\sqrt{\mu_{ij}/\mu_k}$ where $\mu_k =$

$m_k(m_i + m_j)/\sum_l m_l$, and performing the integrals involved in (6), the amplitude T reads

$$T = T^{\text{asy}} + C \int_0^{\pi/2} d\alpha \sin^2 2\alpha T^{\alpha}, \tag{8}$$

where $C = \mathcal{N} \mu_{ij}^{3/2} \mu_k^{3/2} E^2$ and

$$T^{\alpha} = \langle f \Psi_{\text{par}}(\xi_{1\cdots 6}; \alpha) | W | i \rangle,$$

$$T^{\text{asy}} = \langle (1 - f) \Psi_{\text{par}}(\xi_{1\cdots 6}; k_{ij}) | W | i \rangle. \tag{9}$$

If virtual bound states are included the integral in Eq. (8) contains a sum over these states. From Eq. (8) it is obvious that a transition to an asymptotic state defined by the measured momenta $\mathbf{k}_{ij}$ occurs via an infinite number of intermediate virtual transitions, given by T^{α}, which may interfere to result in the measured cross section.

The present method is applicable to an arbitrary three-body Coulomb system. Here we investigate the one-photon double ionization of He($^1S^e$) (DPI) and include in the integral (6) continuum states only. As momentum-exchange effects occur at shorter distances ($R < R_w$) the velocity form of the dipole operator is employed (first-order perturbation theory for the radiation field is assumed). Neglecting energy exchange between the two-body subsystems results in the approximation $\Psi_{\text{ex}} = \Psi_{\text{par}}$, which has been employed for the calculations of the relative angular distributions of electrons following DPI with remarkable success [11,12]. From Figs. 1(a) and 1(b) it is evident that energy-exchange effects strongly depend on the configuration in which the two electrons are emitted. A drastic influence is observed when the two electrons escape with low and asymmetric energies [Fig. 1(b)] in which case the symmetry of the initial-state ($^1S^e$) and the final-state electronic repulsion imposes less severe restrictions on the angular distribution than in the case of equal-energy electrons [12]. In Fig. 2 the electron- and positron-impact ionization of atomic hydrogen is considered. For electron impact the approximation $H - H_{\text{par}} = 0$ leads to some discrepancy between theory and experiment in the binary region. The recoil regime is well described. The present model provides no evidence for two additional shoulders predicted by the convergent close coupling (CCC) calculations [13]. Differences between electron and positron impact as observed in Fig. 2 can be traced to final-state interactions. For proton and antiproton impact [Figs. 3(a) and 3(b)] the projectile is mainly scattered into the forward direction and different

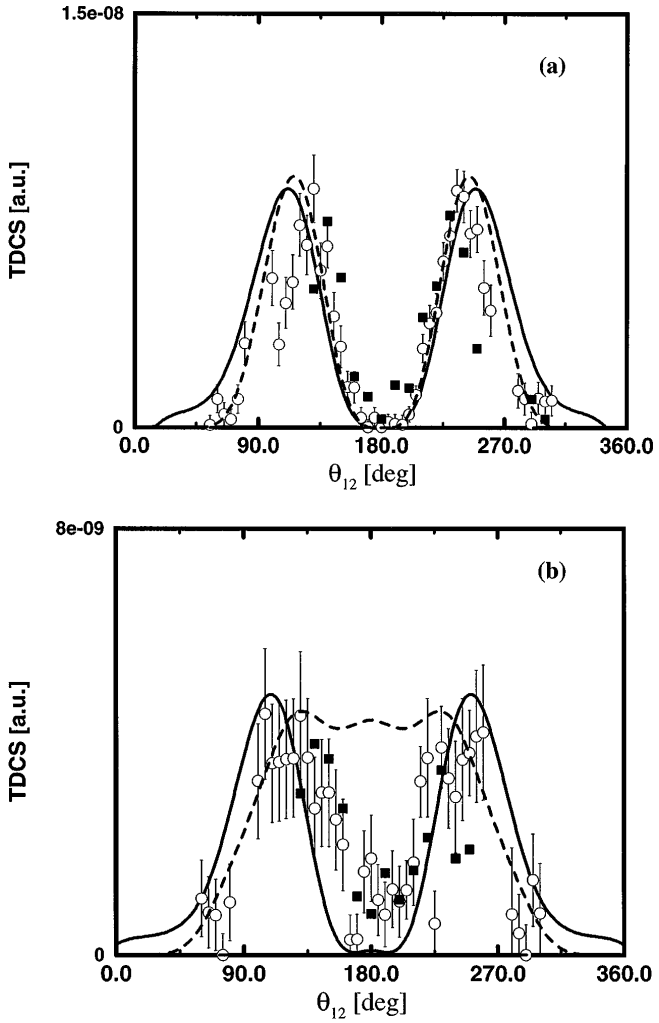

FIG. 1. (a) The triply differential cross section (TDCS) for the double ionization of He($^1S^e$) by a linearly polarized photon. One electron is detected along the direction of the polarization vector (ϵ) while the other electron is detected, in coincidence with the first one, under an angle θ_{12} with respect to ϵ. The two equal-energy electrons escape with a total excess energy of 4 eV. The relative experimental data are due to [16]. Representing the final state by Eq. (7) [or $\Psi_{\text{ex}} \approx \Psi_{\text{par}}$] results in the solid [dashed curve scaled down by 1.8]. The initial state is represented by a Hylleraas wave function which contains radial and angular correlations. (b) The same as in (a) but the electron fixed to ϵ is detected with an energy of 3.3 eV.

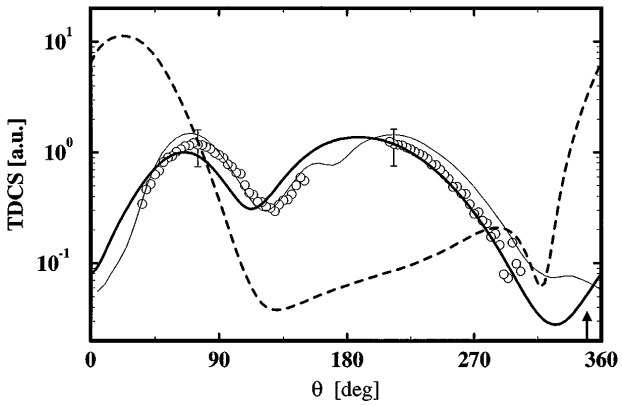

FIG. 2. The TDCS for the coplanar electron-impact ionization of atomic hydrogen calculated using the wave function (7) (solid curve). The incident energy is 54.4 eV. One electron is detected under an angle of 350° with respect to the incident direction $\mathbf{k}_i$, whereas the other one is detected under an angle θ with respect to $\mathbf{k}_i$ and with an energy of 5 eV. Experimental data are due to Ref. [17] with error bars indicating the uncertainty in the absolute value. The CCC results (solid light curve) are taken from Ref. [13] where comparison with a number of other models is made. Predictions of the present study for positron impact are included (dashed curve).

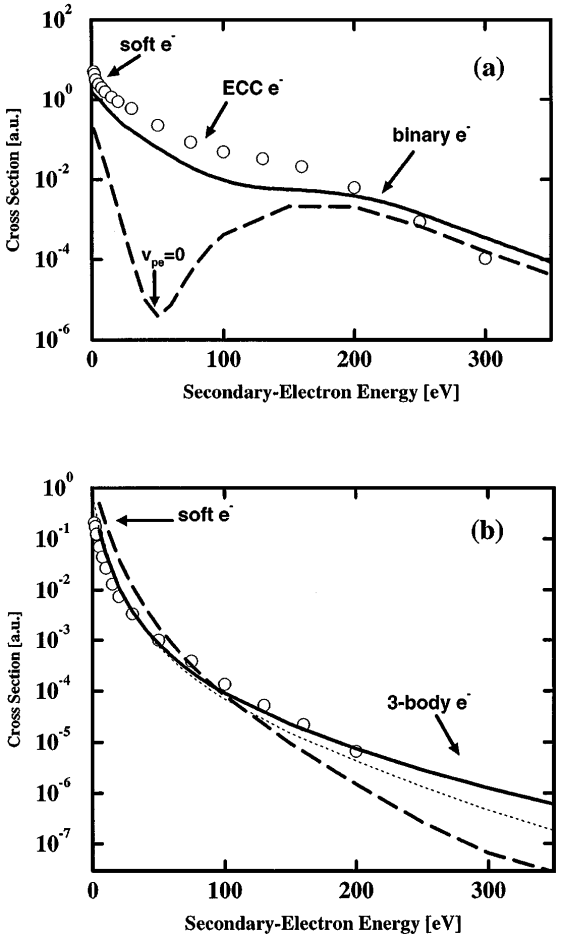

FIG. 3. The energy spectrum of secondary electrons ejected from atomic hydrogen upon proton (solid curve) and antiproton (dashed curve) impact with incident energy of 95 keV. In (a) the electrons are detected at an angle of 15° with respect to the incident beam, whereas in (b) this angle is fixed to 150°. In (b) calculations using $\Psi_{ex} \approx \Psi_{par}$ are included (dotted curve). The absolute experimental data are due to Ref. [18] where comparison with other theories can be found.

ionization mechanisms are distinguished via the particles' relative velocities (since $Z_{ij} = \pm 1$). The most notable difference between proton and antiproton impact appears at a diminishing relative velocity vector $\mathbf{v}_{pe}$ of projectile-electron system [Fig. 3(a)]. This is due to the decisively different analytical behavior of the projectile-electron density of state which, for $v_{pe} \to 0$, is of the form $\exp(-1/v_{pe}) \to 0$ for antiproton and $1/v_{pe} \to \infty$ for proton impact [14,15]. The ridge structure in Fig. 3(a) which appears at an electron velocity equal to twice the projectile's velocity (in the target frame) is due to a direct projectile-electron encounter [14]. Energy-exchange effects are prominent in the region where a high-energy electron is ejected backwards [Fig. 3(b)]. In this case the electron cannot be viewed as emitted in the field of the target (slow soft electrons) nor in the field of the projectile [electrons captured into the projectile's continuum (ECC), ECC electrons with $v_{pe} \to 0$]. Detailed study showed that these electrons are ejected via multiple scattering from both nuclei in events with large deflection of the projectile.

In conclusion, transitions into two-body virtual states have been included for the first time into analytical correlated three-body wave functions with correct asymptotic behavior. To elucidate the effect of these transitions, scattering amplitudes for photo-double ionization and electron, positron, proton, and antiproton-impact ionization leading to three-body continuum final state have been calculated.

I am grateful to S. Buckman, E. Weigold, M. Hoogerland, and S. Mazevet for helpful comments and to A. Huetz for communicating his data. This work was supported by the Alexander von Humboldt Foundation and the Australian National University.

[1] L. Rosenberg, Phys. Rev. D **8**, 1833 (1973).
[2] M. Brauner, J. S. Briggs, and H. Klar, J. Phys. B **22**, 2265 (1989).
[3] E. O. Alt and A. M. Mukhamedzhanov, Phys. Rev. A **47**, 2004 (1993).
[4] J. Berakdar, Phys. Rev. A **53**, 2314 (1996); **54**, 1480 (1996); Phys. Lett. A **220**, 237 (1996).
[5] G. Wannier, Phys. Rev. **90**, 817 (1953).
[6] A. R. P. Rau, Phys. Rev. A **4**, 207 (1971); Phys. Rep. **110**, 369 (1984).
[7] H. A. Bethe and E. E. Salpeter, *Quantum Mechanics of One- and Two-Electron Atoms* (Springer, Berlin, 1957).
[8] J. Berakdar and J. S. Briggs, Phys. Rev. Lett. **72**, 3799 (1994); J. Phys. B **27**, 4271 (1994); **29**, 2289 (1996).
[9] K. A. Berrington, P. G. Burke, K. Butler, M. J. Seaton, P. J. Storey, K. T. Taylor, and Yu Yan, J. Phys. B **20**, 6379 (1987).
[10] T. Kato, Commun. Pure Appl. Math. **10**, 151 (1957).
[11] F. Maulbetsch, M. Pont, J. S. Briggs, and R. Shakeshaft, J. Phys. B **28**, L341 (1995).
[12] F. Maulbetsch, Ph.D. thesis, Freiburg University, 1995.
[13] I. Bray, D. A. Konovalov, I. E. McCarthy, and A. T. Stelbovics, Phys. Rev. A **50**, R2818 (1994).
[14] P. D. Fainstein, V. H. Ponce, and R. D. Rivarola, J. Phys. B **24**, 3091 (1991).
[15] J. Berakdar, J. S. Briggs, and H. Klar, Z. Phys. D **24**, 351 (1992).
[16] A. Huetz, L. Andric, A. Jean, P. Lablanquie, P. Selles, and J. Mazeau, in *Proceedings of XIX International Conference on the Physics of Electronic and Atomic Collisions, Whistler*, edited by L. Dube' *et al.* (AIP Press, New York, 1995).
[17] J. Röder (private communication).
[18] G. W. Kerby III, M. W. Gealy, Y.-Y. Hsu, and M. E. Rudd, Phys. Rev. A **51**, 2256 (1995).